Fuel 333 (2023) 126478

Contents lists available at ScienceDirect

Fuel

journal homepage: www.elsevier.com/locate/fuel

Full Length Article

CH_4 adsorption and diffusion characteristics in stress-loaded coal based on molecular simulation

Hai-fei Lin [a,b,*], Hang Long [a,b], Shu-gang Li [a,b], Yang Bai [a,b,*], Tong Xiao [a,b], Ao-li Qin [a,b]

[a] School of Safety Science and Engineering, Xi'an University of Science and Technology, Xi'an, Shaanxi 710054, China
[b] Western Coal Gas Disaster Prevention Engineering Research Center, Ministry of Land and Resources of the People's Republic of China, Xi'an, Shaanxi 710054, China

ARTICLE INFO

Keywords:
Molecular simulation
Micro- and meso-porous slit models
Stress-strain characteristics
Adsorption characteristics of CH_4
Diffusion coefficient and type

ABSTRACT

The Variety of roof stress during mining was one of the main factors affecting the adsorption and diffusion characteristics of coalbed methane. CH_4 adsorption and diffusion characteristics in micro- and meso-pores of coal under different stress loading were simulated in this study by means of molecular mechanics and molecular dynamics. Firstly, the micro- and meso-pores of coal with four different slit widths (10 Å, 20 Å, 50 Å, and 80 Å, respectively) were established. Then, the stress-strain characteristics of the frameworks under different stress loading were studied by applying uniaxial stress. Finally, the CH_4 adsorption and diffusion characteristics in different stress-deformed frameworks were investigated. Under the action of stress loading, the mesoporous framework showed a stronger deformation tendency. This process can be divided into the deformation occurring in the coal molecule and the slit. The energy evolution of coal framework under stress presented an exponential decay trend, which resulted in a decreasing trend in the adsorption amount of CH_4 in the framework. Under the loading of 10 GPa external stress, the CH_4 absolute adsorption amount in the four frameworks decreased by 65.21 %, 65.21 %, 68.07 %, and 70.98 %, and the excess adsorption amount decreased by 54.33 %, 69.07 %, 69.75 %, and 73.85 %, respectively, compared with the initial framework ($\sigma = 0$ GPa). The absolute adsorption amount and self-diffusion coefficient of CH_4 both increased with the increasing slit width. In the compression stage of the framework, the heat released by CH_4 adsorption showed a decreasing trend, and the self-diffusion coefficient of CH_4 showed an increasing trend. However, in the stage of slit compression, the adsorption heat and self-diffusion coefficient tended to increase and decrease, respectively. By analyzing the diffusion types of CH_4 in micro- and meso-pores, it was found that, in micropores, transitional and Knudsen diffusion were dominant, while in mesopores, transitional and Fick diffusion were dominant. This study can provide theoretical reference for coal seam gas pre-extraction engineering.

1. Introduction

As an important unconventional natural gas resource, coalbed methane (CBM) has attracted extensive attention in China due to its abundant reserves and high utilization efficiency [1,2]. However, the complex transmission mechanism and geological conditions resulted in a low recovery rate of the reservoir. Therefore, enhanced gas recovery is very necessary for CBM reservoir development [3]. Pre-extraction of CBM before mining is a common method to recover gas resource. Before the working face is mined, the coal seam is in a state of equal stress in three directions [4]. With the coal seam mining, the changes in external stresses lead to compressed deformation of the pores and slits [5], which in turn affects the adsorption and diffusion of gases, leading to discrepancies in the rational arrangement of the CBM extraction process. Therefore, studying the closed state of pores and the characteristics of gas adsorption under different stress states is the basis for the rationalization of gas extraction technology.

Molecular dynamics (MD) simulation was often used to study the microscopic mechanism between adsorbents and adsorbates [6,7]. Han [8] and Li [9] utilized Molecular simulations to carried out CH_4/CO_2 competitive adsorption and diffusion in moisture coals. Sharma [10] studied the structural and dynamical properties of CH_4 and C_2H_6 in different montmorillonite (MMT) slit pore using grand canonical Monte Carlo (GCMC) and MD simulations. Zhu [11] and Gao [12] considered

* Corresponding authors at: School of Safety Science and Engineering, Xi'an University of Science and Technology, 58, Yanta Mid. Rd., Xi'an 710054, Shaanxi, PR China.
E-mail addresses: lhaifei@xust.edu.cn (H.-f. Lin), 978486384@qq.com (Y. Bai).

https://doi.org/10.1016/j.fuel.2022.126478
Received 28 July 2022; Received in revised form 4 October 2022; Accepted 21 October 2022
Available online 29 October 2022

the influence of temperature on lignite structure, and analyzed the flow characteristics of different gases by GCMC. Tesson [13] investigated CH_4 adsorption in kerogen frameworks with different surface roughness at different temperatures and pressures by utilizing MD simulation. Tolmachev [14] and Li [15] et al. employed MD methods to analyze the characteristics of gases in slit-like pores of coal.

It is also common to study the micromechanics of molecular frameworks by molecular simulation. Fang [16] investigated the molecular-scale mechanism of the mechanical response of coal under different external stresses. The results showed that, as the stress increased, the density of the unit cell gradually increased, the methane adsorption performance and overall system energies of the unit cell decreased. Mohammadi [17] investigated the mechanical properties of twin graphene sheets by applying uniaxial stress, and it was found that Young's modulus decreased with increasing the size and temperature of system. Wu [18] derived a working expression for estimating the free energy of the solid–fluid interface based on the perturbation method considering solid deformation, and the results revealed that the contribution of the solid deformation highly depends on the stress conditions in the solid. Lin [19] investigated the micromechanical characteristics of medium after CO_2 sequestration by conducting MD-GCMC, mainly included in the Young's modulus, Poisson's ratio and bulk modulus of the coal molecular model after gas adsorption and sequestration.

Based on those, it was feasible to use molecular dynamics and molecular mechanics to study CH_4 adsorption characteristics in coal slit model under different external stresses. Previous studies had mainly focused on gas adsorption characteristics and the mechanical properties of porous media [20,21]. However, in the process of coal mining, the change of ground stress on the coal seam led to the difference in the gas flow and adsorption in coal. Therefore, the molecular simulation was conducted to characterize the adsorption and diffusion of CH_4 in deformed/undeformed model under different stresses in this paper. It can provide theoretical support for coal gas occurrence and gas drainage under different stress states.

2. Computational methodology

2.1. Coal structure units

Coal is a natural porous material with complex physical and chemical structure. The structure units of coal models adopted in this work were built by Wiser (USA) ($C_{184}H_{155}O_{20}N_3S_3$) [22], which was considered to be the most suitable for reflecting the molecular structure of coal. The mass percentages of each element were: C was 78.27 wt%, H was 5.49 wt%, O was 11.34 wt%, N was 1.49 wt%, and S was 3.40 wt% [23]. The Accelrys Materials Studio 7.0 software (http://accelrys.com) was utilized to conduct the mechanical parameters of coal molecule model and the adsorption characteristics of CH_4 in coal.

2.2. Slit model of coal molecules

Coal molecular unit cell model was generated through Amorphous Cell and MD simulations. The molecular potential of Lennard-Jones 6–12 was utilized to describe the dispersive repulsive interactions between pairs of atoms [24]. Moreover, the geometry optimization and dynamics in Forcite module were used to optimize the structure of the model. The geometry optimization parameters were the same as those in Ref. [6]. The final density of coal molecules was 1.3 g/cm^3, which was consistent with the density of bituminous coal (1.2–1.4 g/cm^3) [26]. After structure and energy optimization, a cubic unit cell was obtained with stable structure, lowest energy, periodic boundaries and side length of 15.54 Å. Based on this, the cell was expanded to a $1 \times 2 \times 2$ supercell, and a 10 Å, 20 Å, 50 Å, and 80 Å vacuum layer was added, respectively, and the slit models of coal molecules with different size were obtained. As shown in Fig. 1 was the building procedure of slit model.

2.3. Uniaxial compression

In a small system consisting of several hundred or several thousand atoms, the fluctuation of the model stress was about 0.1 GPa [27]. In this paper, CH_4 adsorption simulations in the coal slit model under different external stresses were carried out, and the schematic diagram of the force was shown in Fig. 2. Firstly, the uniaxial compression simulation of the framework under different external stresses was carried out. The mechanical properties of the framework can be obtained by running a script file in Materials Studio. External stress was applied in the Z direction of the framework, and the X and Y directions were both set as free surfaces (not subject to external stress). The external stress was set from 0 to −10 GPa, and the Gradient was −1 GPa, where the negative values indicated compressive stress. The Time Steps was set to 2000 steps, and the Equilibration and Production were both set to 5000 steps. The Condensed-phase Optimized Molecular Potentials for Atomistic Simulation Studies (COMPASS) forcefield was selected to calculate current Forcefield [15,25]. A total of 10 deformed coal molecular frameworks can be obtained for each slit model.

2.4. Simulation details

Then, the isotherm adsorption of CH_4 in frameworks were simulated. The maximum gas injection pressure was set to 10 MPa, and the gradient was 1 MPa. The atom-based and Ewald method with a cutoff distance of 12.5 Å was utilized to calculated the Van der Waals and Coulombic interactions, respectively [28,25]. The temperature was fixed at 303 K and imposed with the Andersen thermostat. The Charge Equilibration (Q_{Eq}) method was used to calculate the charges. The total simulation steps were set to 2×10^6 steps, of which 1×10^6 steps were used to balance the framework.

The fugacity, which was equal to gas pressure at low pressure, was

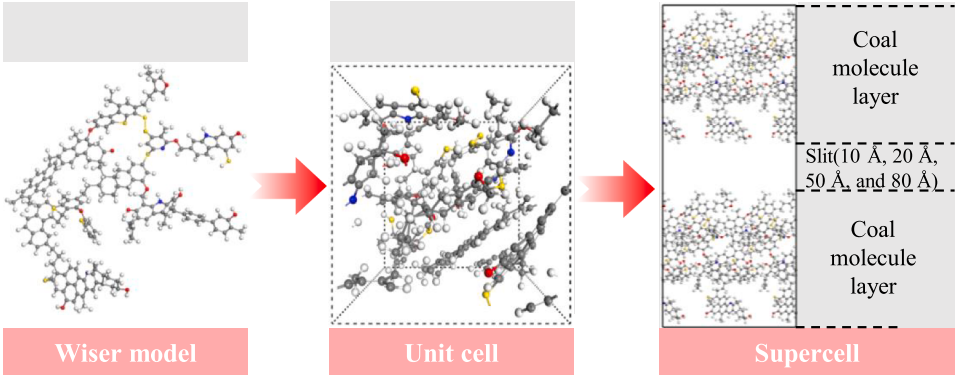

Fig. 1. Building procedure of coal molecular slit model.

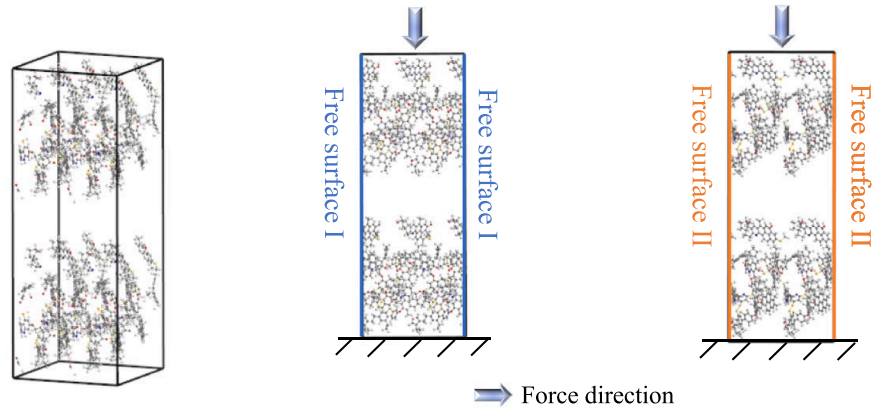

(a) Initial framework (b) Force diagram in X-Z direction (c) Force diagram in Y-Z direction

Fig. 2. Force diagram of the framework under the uniaxial compression.

applied to predict the adsorption amount in the simulations [6]. The relationship between fugacity and pressure was illustrated in Fig. 3 according to Peng-Robinson (PR) equation [29]. The absolute adsorption amount of gas molecules can be obtained, and all the absolute isotherm adsorption were fitted by the Langmuir model [30].

$$n = \frac{abp}{1 + bp} \tag{1}$$

where n was the gas absolute adsorption amount, N/cell. a was the extreme adsorption amount, N/cell. b was the pressure constant, 1/MPa. p was the pressure, MPa. The excess adsorption amount was computed [31,32].

$$n^e = n(1 - c) \tag{2}$$

where n^e was the excess adsorption capacity, N/cell. c was the relative concentration of CH_4 in the slit.

2.5. Gas self-diffusion

Mean square displacement (*MSD*) was one of the main methods to analyze gas diffusion characteristics in molecular simulation. When the system was in a solid state, that was, the temperature of the system was below the melting point, the *MSD* had an upper limit. When the system was in a liquid state, the *MSD* had a linear relationship with time τ, and its slope had the following relationship with the molecular diffusion coefficient [33,34].

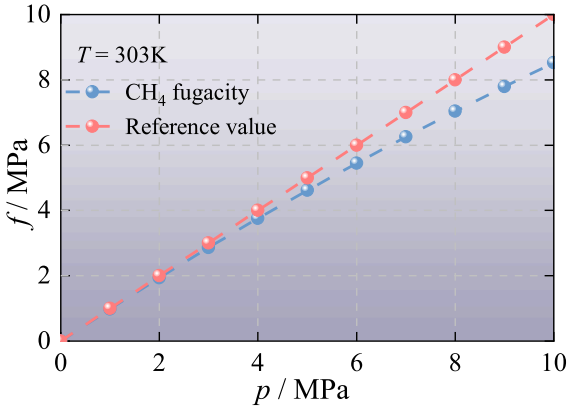

Fig. 3. Conversion relationship between fugacity and pressure of CH_4 at 303 K.

$$D = \frac{1}{6}\lim_{\Delta\tau\to\infty}\frac{\mathrm{d}MSD}{\mathrm{d}\Delta\tau} \tag{7}$$

where D was the self-diffusion coefficient, $m^2 \cdot s^{-1}$. Gas molecule diffusion was equivalent in 6 directions, so the coefficient was 1/6 in a cubic lattice.

From the point of view of molecular motion, the essence of gas diffusion was the result of irregular thermal motion of gas molecules. The diffusion type of gas molecules in different pore can be judged according to the Knudsen number (K_n), which was usually divided into Fick, transitional and Knudsen type. The diffusion was Fick type if $K_n \geq 10$, where the pore diameter (d) was much larger than the mean free path of pore gas molecules (λ), and the collision of gas molecules mainly occurred between gas molecules in free pore. When $0.1 < K_n$ less than 10, it was transitional type, where the mean free path of gas molecules in pore was similar to the pore diameter, and the collision between molecules was equally important as the collision between molecules and the wall. When $K_n \leq 0.1$, the diffusion was Knudsen type, and the mean free path of the molecules was larger than the pore diameter, and the collisions between gas molecules and the pore walls dominated. The expression of K_n was shown as follows [35].

$$\begin{cases} K_n = \dfrac{d}{\lambda} \\ \lambda = \dfrac{\kappa_B T}{\sqrt{2}\,\pi d_0^2 p} \end{cases} \tag{8}$$

where κ_B was Boltzmann constant, 1.38×10^{-23} J/K. T was absolute temperature, K. d_0 was the effective diameter of gas, nm.

3. Result and discussion

3.1. Stress–strain curve and energy evolution of model

The different stresses were applied along the vertical direction of models, the stress range was from 0 to −10 GPa, and the gradient was −1 GPa. A total of 16 stress–strain curves were obtained, and each group contained 11 data points. As shown in Fig. 4, the X, Y, Z directions and volume strains of the coal model with different slit widths under different stresses were illustrated respectively, where the positive values represented compression deformation, and the negative ones represented expansion. Under the action of external stress, coal molecules exhibited compression deformation along the stress direction, and expansion deformation occurred in the direction of the free surfaces on both sides, which was consistent with the research results in Ref. [19].

In view of Fig. 4(a) and (b), with the gradual increase of the external

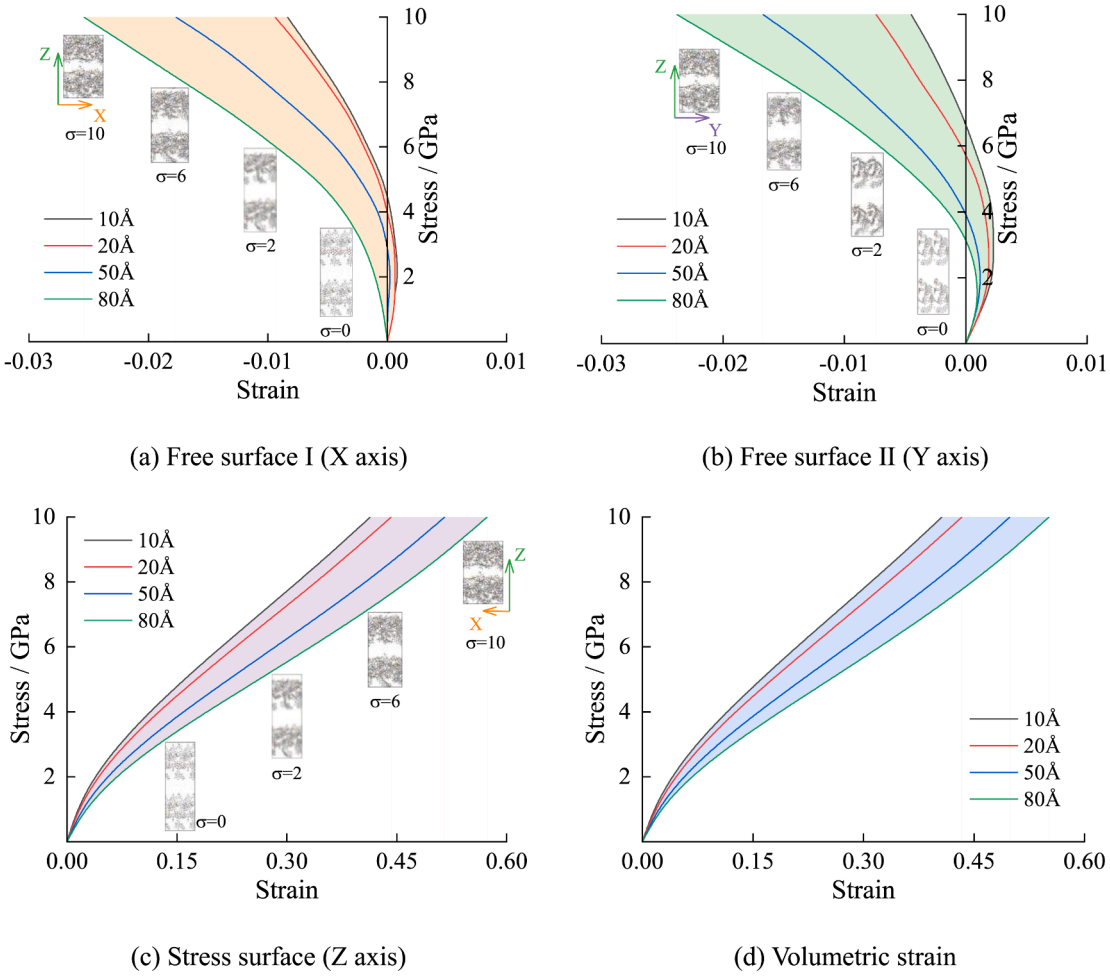

Fig. 4. Stress–strain characteristics of different coal slit models.

stress, the different degrees of expansion deformation were occurred in the free surface. Coal molecular models with larger slit widths were more prone to deformation. The strains in the X and Y directions of the coal molecular model with 10 Å slit width in the simulated stress range reached 0.008 and 0.004, and those of the 80 Å model was 0.025 and 0.024, respectively.

As shown in Fig. 4(c) and (d), the coal molecular model generally exhibited compressive deformation under the action of external stress, mainly including the deformation of the coal molecular layer and the slit. The coal molecular model with larger slit width was more prone to be compressed. When the slit width was 10 Å, the strain of the model along the stress applied direction was 0.41, and the volumetric strain was 0.41. For a model with a slit width of 80 Å, the strain of the model along the stress and the volumetric strain were 0.57 and 0.52 respectively. In the initial stage of external stress, coal molecules first showed a compacted state. The deformation of the coal molecular layer dominated the overall deformation of model. The slits in the model gradually collapsed as the stress increased.

As shown in Fig. 5, the energy evolution of the coal unit cell model with different slit widths under different stresses were analyzed. As the external stress increased, the energy in the coal unit cell model exhibited an exponential decay. The larger the slit width was, the more obvious the energy attenuation was. According to the principle of minimum energy, systems with lower energies were more likely to exhibit stable states. Non-bonding energy mainly referred to the interaction energy between coal molecules in the system. Before external stress applying, the energy of coal molecular unit cell system was higher. Under the action of external force, the interaction energy between coal molecules

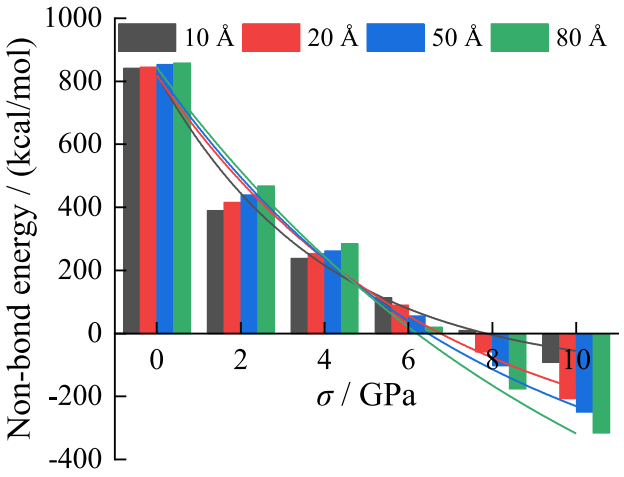

Fig. 5. Energy evolution of unit cells under different stresses.

decreased rapidly, indicating that the compression deformation of coal molecular layer was the main factor in the initial stage of stress application. With the increasing external stress, the energy between coal molecules gradually decreased, the effect of stress on the compression of coal molecular layer gradually decreased, and the deformation of coal unit cell was gradually affected by the slit compression.

3.2. CH_4 adsorption amount

The adsorption characteristics in the slit model were explored before and after external stress loading. The results were illustrated in Fig. 6, and the isotherm adsorption amount were fitted by Langmuir equation. The process of CH_4 adsorption in the framework mainly experienced the change trend of rapidly, slowly, and gently increase. As shown in Fig. 6, the absolute amount of CH_4 adsorption mainly included the sum of the adsorption amount in the coal molecular layer and the gas loading in the slit. Before external stress loading, the larger the slit width, the more the absolute adsorption amount in the framework. Under the action of external stress, the slit of framework and the coal molecular layer gradually compressed, resulting in a decrease in the absolute adsorption amount of CH_4. Compared to the framework unloaded external stress, the absolute adsorption amount of CH_4 in the slit framework of 10 Å, 20 Å, 50 Å and 80 Å was reduced by 65.21 %, 65.21 %, 68.07 %, and 70.98 % under the gas pressure of 10 MPa, respectively. It indicated that the compression effect of external stress had a significant effect on the absolute adsorption amount of CH_4 in the coal framework [16].

Fig. 6 CH_4 adsorption characteristics in different coal slit models under various stress.

The fitting results of the Langmuir-type equation of the experimental data were illustrated in Table 1. The extreme adsorption amount a of CH_4, which was represented the maximum loading amount in the framework, increased with the increase of slit width. The pressure constant b showed a decreasing trend with the increase of the slit width. Meanwhile, the extreme adsorption amount decreased with the increasing external stress, and b firstly decreased and then increased with the increase of stress loading in a specific slit framework.

3.3. Isosteric heat of adsorption

Isosteric heat of adsorption was one of the important indicators to measure the adsorption characteristics of adsorbents, which was the thermal effect generated during the adsorption process. When the gas was adsorbed in the framework, it overcome the interaction force between the gas and the solid, so a certain amount of heat need to be released. As shown in Fig. 7 was the isosteric heat of CH_4 adsorption in the various slit framework under different external stresses. With the increase of the absolute adsorption amount of CH_4 in the framework, the isosteric heat of adsorption generally showed a decreasing trend. Under the same stress, the heat released by CH_4 adsorption in the framework decreased with the increase of slit width. With the increase of external stress, the adsorption heat of CH_4 in the framework generally showed a trend of first decreasing and then increasing, which was consistent with the change of pressure constant b.

3.4. Excess adsorption amount

The adsorption simulation mainly obtained the maximum amount of CH_4 that can be adsorbed in the framework, that was, the absolute adsorption amount. The absolute adsorption amount included the gas molecules adsorbed in the coal molecule layer in the form of adsorption phase, and the gas molecules existing in the slit of the framework in the form of free phase. In practice, the excess adsorption amount was used for comparison, that was, only the gas molecules that were adsorbed on

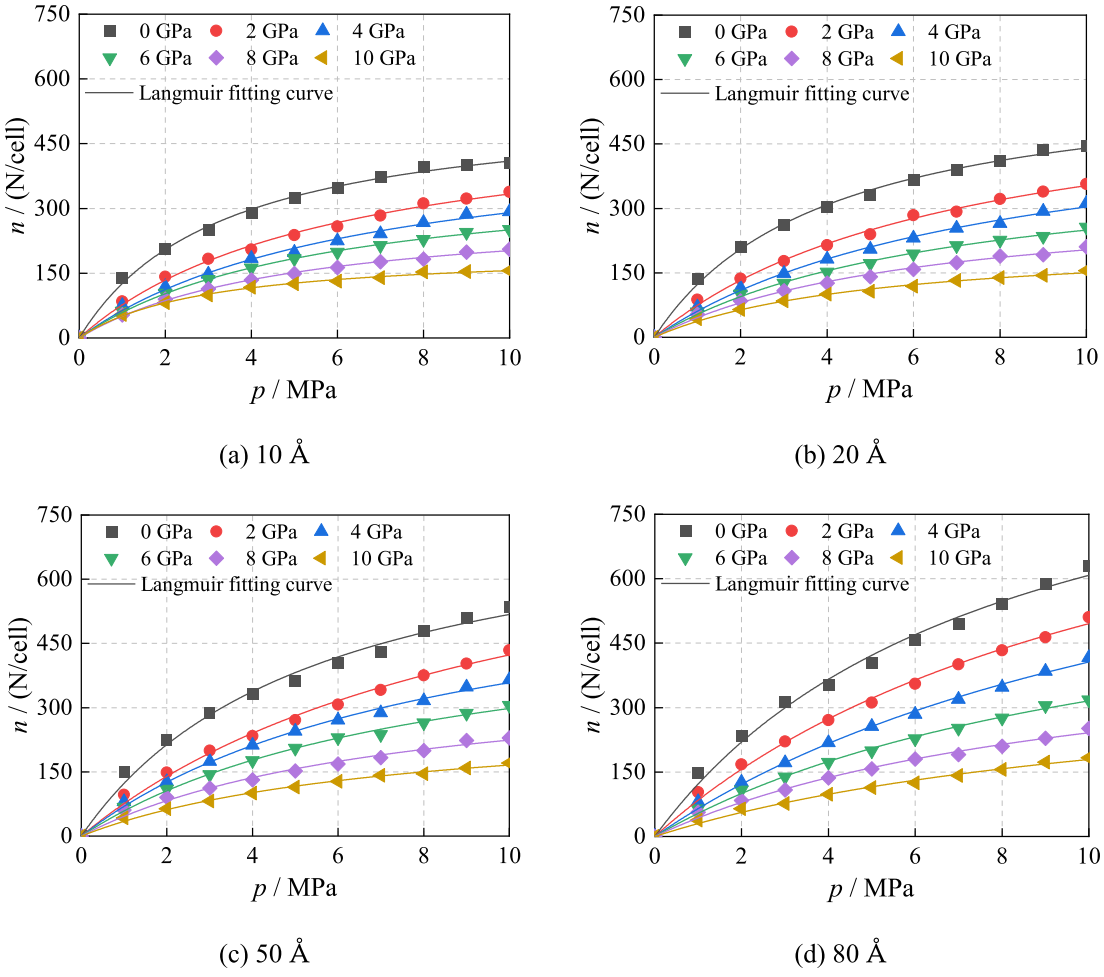

Fig. 6. CH_4 adsorption characteristics in different coal slit models under various stress.

Table 1
The fitting result of CH_4 absolute adsorption in different slit under various stress.

Width	Stress	*a*	*b*	R^2	Width	Stress	*a*	*b*	R^2
10 Å	0	546.39	0.30	99.67 %	20 Å	0	616.80	0.25	99.72 %
	2	530.83	0.17	99.58 %		2	603.15	0.14	99.63 %
	4	480.27	0.15	99.42 %		4	545.42	0.13	99.64 %
	6	391.34	0.18	99.92 %		6	421.37	0.15	99.69 %
	8	303.61	0.20	99.80 %		8	329.69	0.16	99.45 %
	10	202.62	0.34	99.69 %		10	226.49	0.20	99.48 %
50 Å	0	803.06	0.18	99.10 %	80 Å	0	1087.94	0.13	99.24 %
	2	758.70	0.10	99.47 %		2	1078.54	0.08	99.61 %
	4	665.49	0.12	99.69 %		4	977.17	0.07	99.66 %
	6	544.71	0.12	99.62 %		6	684.70	0.09	99.64 %
	8	392.20	0.13	98.85 %		8	490.88	0.10	99.28 %
	10	287.63	0.14	99.51 %		10	398.43	0.10	99.28 %

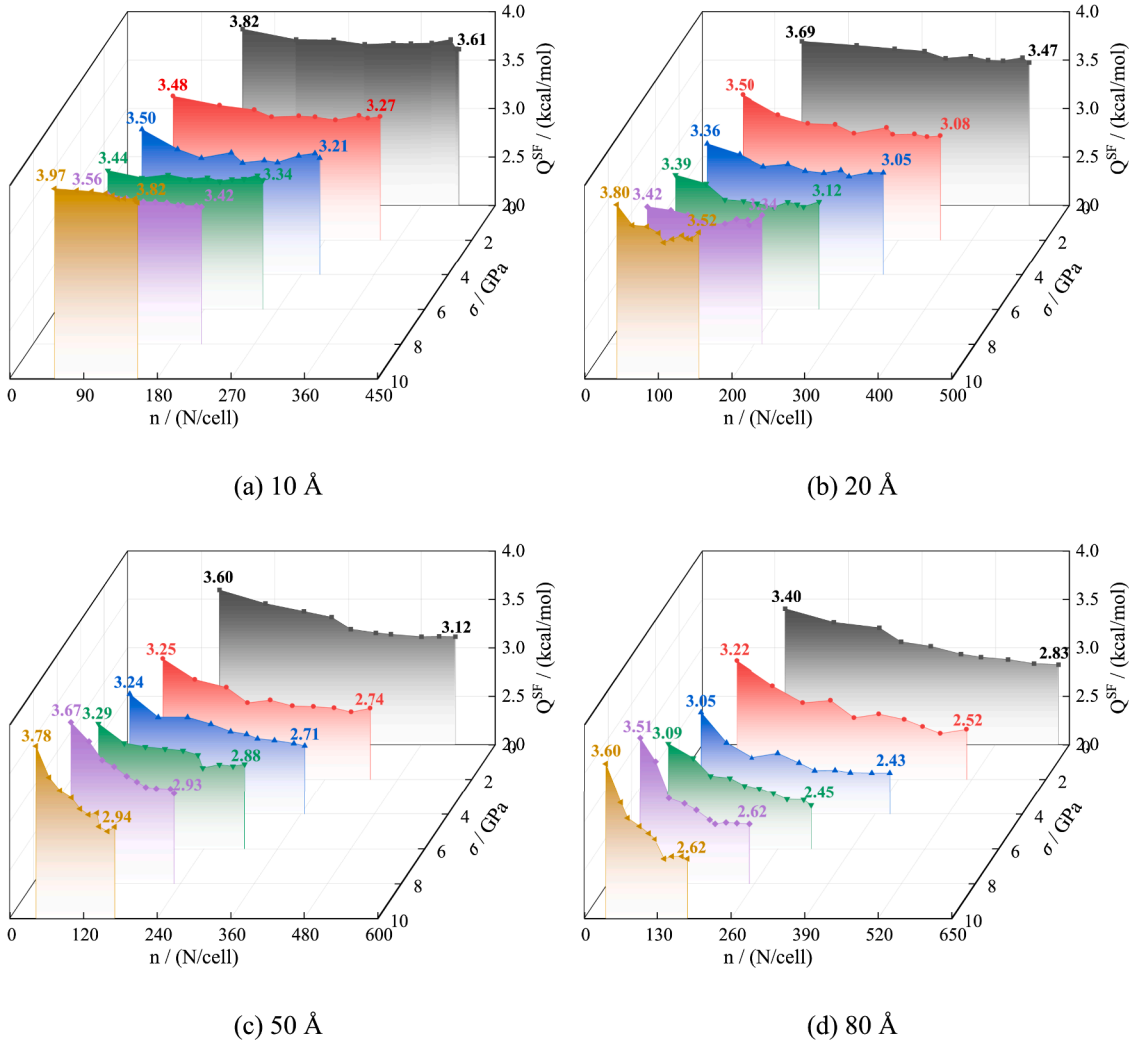

Fig. 7. Variation of adsorption heat in the process of CH_4 adsorption.

the coal molecule layer in the form of adsorption phase. In order to obtain the excess adsorption amount in the framework under different stresses, it was necessary to count the number of CH_4 molecules in the slit. Firstly, the overall size of the framework and the size of the coal molecular layer were determined, and then the slit width parameters under different stresses were obtained. Secondly, by means of molecular dynamics, the relative concentration of CH_4 in the slit was determined. As shown in Fig. 8, the red frames were the range of slit under various external stress, and the black lines indicated the relative concentrations of CH_4 in the framework.

According to the analysis of the relative concentration of CH_4 in the coal molecular layer and the slit in the framework, the relative adsorption amount of CH_4 under the gas pressure of 10 MPa was determined as shown in Fig. 9. As shown in Fig. 9(a), increased the slit width can provide more space for CH_4 adsorption in the framework. The absolute adsorption amount of CH_4 at 10 MPa showed a decreasing trend with stress loading. Whereas the excess adsorption amount of CH_4 showed a decreasing trend with the increasing of slit width (Fig. 9(b)), which was consistent with the conclusion that CH_4 adsorption mainly occurs in the micropores [6]. Compared to the framework unloaded

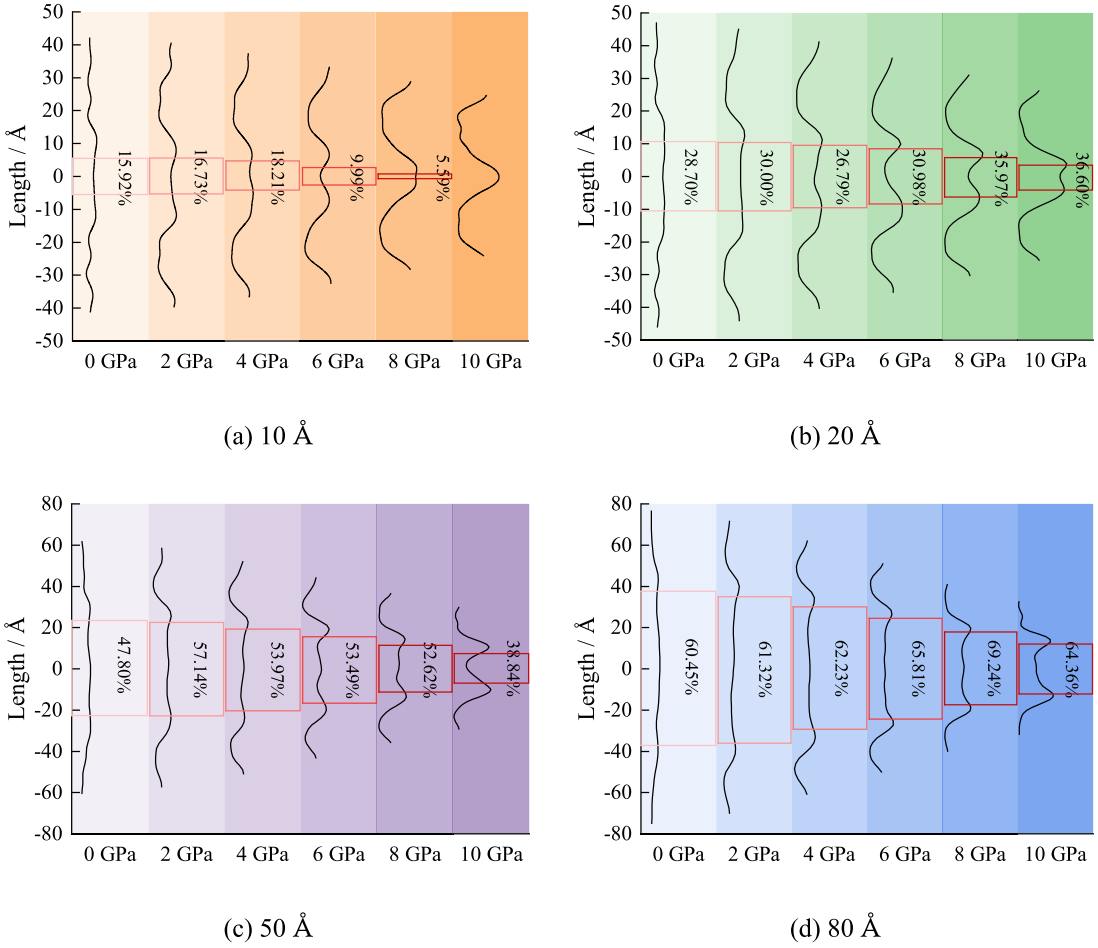

Fig. 8. Variation of CH_4 concentration in the slit under external stress.

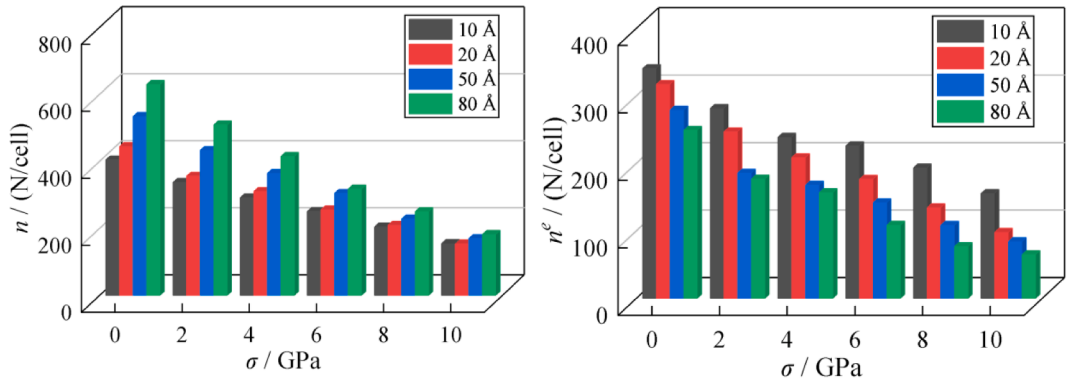

Fig. 9. Adsorption amount of CH_4 in stress-deformed coal (p = 10 MPa).

external stress, the excess adsorption amount of CH_4 in the coal molecular layer of four frameworks was reduced by 54.33 %, 69.07 %, 69.75 %, and 73.85 % under the gas pressure of 10 MPa, respectively. In the micropores, the van der Waals potential generated by the pore walls overlapped, resulting in the force of the coal molecular layer on the gas molecules in the micropores was greater than that in the mesopores. As shown in Fig. 5, the energy in the framework decreased with the stress loading, leading to a more stable system. CH_4 entered the stress-deformed framework, and the lower energy system will provide fewer adsorption sites, thus leading to a decrease in the adsorption capacity of CH_4.

3.5. *The self-diffusion of CH_4*

Mean Square Displacement (MSD) analysis was a technique for determining particle displacement patterns over time. In particular, it can help determine whether particles were free to diffuse, transport or bind. In addition, MSD analysis can produce estimates of motion

parameters, such as the diffusion coefficient of freely diffusing particles.

As illustrated in Fig. 10 was the relationship between MSD and simulation time τ, whose slope represented the self-diffusion coefficient of CH_4 in the framework. With the increase of external stress, the slope of MSD and time showed a trend of increasing first and then decreasing, and the slope was the largest when the external stress was 4 GPa. According to Eq.(7), the calculated results of the self-diffusion coefficients of CH_4 in different slit framework under various stresses were shown in Table 2.

With the increase of the slit width, the self-diffusion coefficient of CH_4 in the framework generally showed an increasing trend. With the increase of the external stress, it showed a trend of first increasing and then decreasing, reaching the maximum when the external stress was 4 GPa. The maximum CH_4 self-diffusion coefficients in the four frameworks were 2.62×10^{-8}, 3.62×10^{-8}, 6.35×10^{-8} and 9.06×10^{-8} $m^2 \cdot s^{-1}$, respectively. It indicated that larger slit width can provide more space for CH_4 diffusion.

According to the calculation of the Knudsen number of CH_4 in different frameworks under various stresses, the diffusion type of CH_4 under different conditions was determined as shown in Table 3. Under the simulation conditions, most of the CH_4 diffusion was transitional, that was, there were both Fick and Knudsen diffusion. In the 10 Å slit framework, with the increase of stress, the diffusion type of CH_4 gradually transferred from transition type to Knudsen type. In the initial framework, since the mean free path of CH_4 was close to the slit width, there was a certain probability that the molecule will collide with the pore wall, which was a transitional diffusion process. As the external stress increased, the slits of the framework gradually compressed, resulting in an increase in the probability of collision between CH_4 molecules and the pore wall, and the diffusion type was transformed from transitional type to Knudsen type.

In the 80 Å slit framework, since the slit width of the initial framework was much larger than the molecular mean free path of CH_4, CH_4 hardly collided with the pore wall during it moved in the framework. As the external stress increased, the slit width of the framework gradually decreased to approach the molecular mean free path of CH_4, resulting in

Table 2
Self-diffusion coefficients of CH_4 in different slit under various stresses.

Width	σ	Slope	D / ($\times 10^{-8}$ $m^2 \cdot s^{-1}$)	Width	σ	Slope	D / ($\times 10^{-8}$ $m^2 \cdot s^{-1}$)
10 Å	0	14.00	2.33	20 Å	0	19.85	3.31
	2	15.41	2.57		2	21.17	3.53
	4	15.72	2.62		4	21.74	3.62
	6	11.96	1.99		6	19.77	3.30
	8	9.12	1.52		8	13.07	2.18
	10	4.09	0.68		10	11.42	1.90
50 Å	0	30.37	5.06	80 Å	0	40.51	6.75
	2	37.12	6.19		2	48.12	8.02
	4	38.11	6.35		4	54.36	9.06
	6	33.00	5.50		6	48.04	8.01
	8	32.17	5.36		8	42.96	7.16
	10	22.60	3.77		10	31.81	5.30

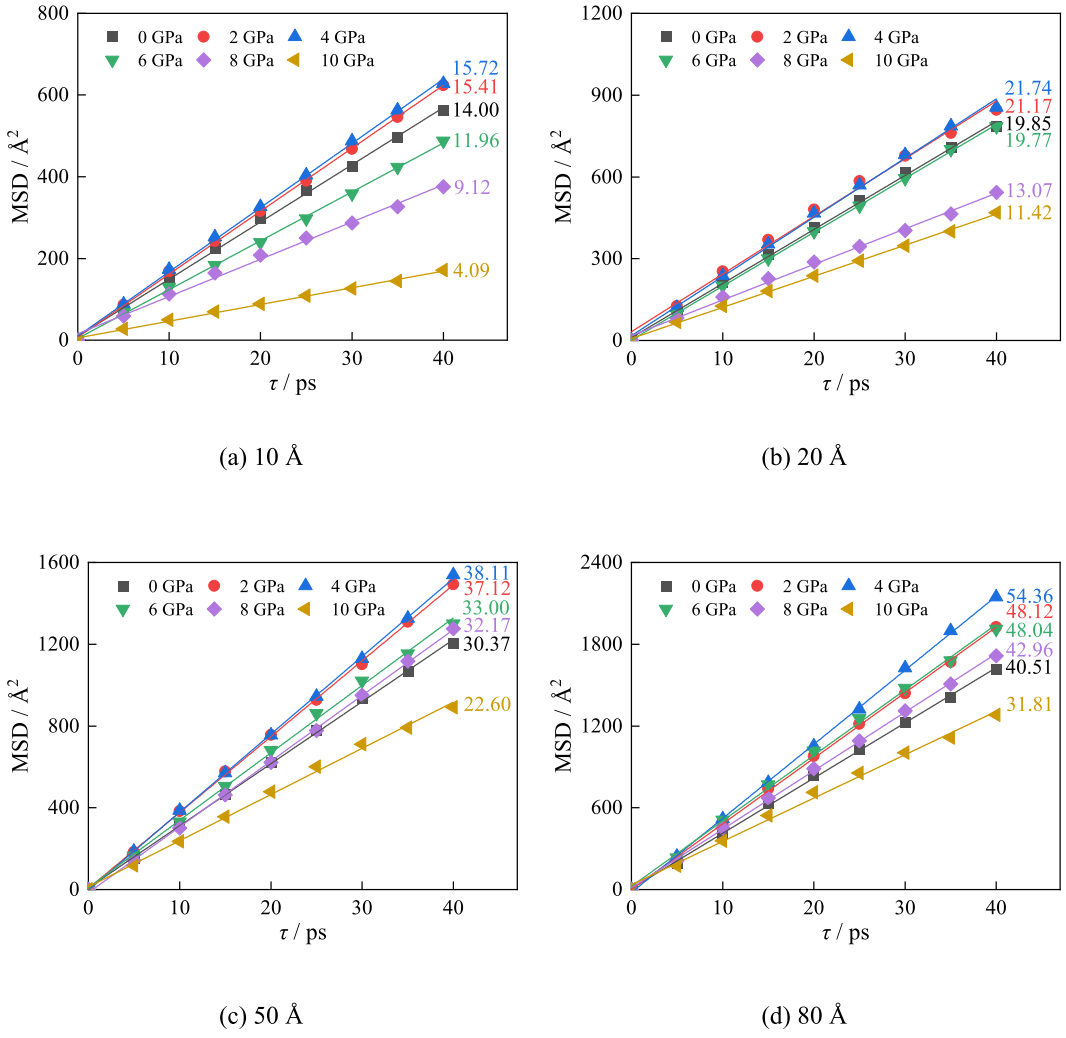

Fig. 10. MSD of CH_4 in stress-deformed coal (p = 10 MPa).

Table 3
Analysis of diffusion types in different slit under various stresses.

Width	σ / GPa	d / nm	K_n	Type	Width	σ / GPa	d / nm	K_n	Type
10 Å	0	1.153	2.10	Transitional	20 Å	0	2.155	3.92	Transitional
	2	1.103	2.01	Transitional		2	2.079	3.78	Transitional
	4	0.958	1.74	Transitional		4	1.929	3.51	Transitional
	6	0.57	1.04	Transitional		6	1.729	3.15	Transitional
	8	0.106	0.19	Knudsen		8	1.257	2.29	Transitional
	10	0	0	Knudsen		10	0.743	1.35	Transitional
50 Å	0	5.159	9.39	Transitional	80 Å	0	8.162	14.85	Fick
	2	5.101	9.28	Transitional		2	7.702	14.02	Fick
	4	4.469	8.13	Transitional		4	6.487	11.81	Fick
	6	3.637	6.62	Transitional		6	5.38	9.79	Transitional
	8	2.542	4.63	Transitional		8	3.891	7.08	Transitional
	10	1.669	3.04	Transitional		10	2.7	4.91	Transitional

a gradual increase in the collision probability between the gas and pore wall. At this time, the diffusion type was also converted from Fick type to transitional type.

3.6. Discussion

The adsorption and diffusion characteristics of CH_4 in four frameworks (the slit widths were 10 Å, 20 Å, 50 Å and 80 Å, respectively, mainly included micro- and *meso*-porous frameworks [36]) were researched under various external stresses, as shown in Fig. 11. With the increasing external stress, the framework undergone compressive deformation along the stress loading direction, while expansion deformation occurred in the direction of the two free surfaces. From the change of the framework volume, it can be seen that under the action of stress loading, the framework mainly undergone a compressive deformation.

The absolute adsorption amount of CH_4 in the framework mainly included two parts, one was the adsorption amount of CH_4 in the coal matrix (excess adsorption capacity, n^e), and the other was the loading amount of CH_4 in the slit. With the increase of external stress, the adsorption amount of CH_4 in the framework showed a decreasing trend. This change can be understood from the following two aspects. On the one hand, under the action of stress, the energy of the coal molecular layer gradually decreased and approached a relatively stable state, so the difficulty of CH_4 adsorption in coal increased, resulting in a decrease in the excess adsorption amount of CH_4. On the other hand, the slit width under external stress was reduced, and the pore in the framework was reduced, which can provide the space for CH_4 loading.

By fitting the data with the Langmuir equation, it was found that the adsorption constant a showed a decreasing trend with the increase of stress, which represented the adsorption capacity of CH_4 in the framework. The pressure constant b firstly decreased and then increased with the increase of stress, which represented the difficulty of CH_4 adsorption in the framework. The variation of the pressure constant b showed that when the stress was less than 4 GPa, the adsorption difficulty of CH_4 in the framework gradually decreased as the stress increased. When the stress was greater than 4 GPa, the adsorption difficulty of CH_4 in the framework gradually increased. This change can also be verified from the change law of the adsorption heat, which reflected the difficulty of adsorption from the perspective of thermodynamics. When the stress was less than 4 GPa, the adsorption heat showed a decreasing trend with the increase of the stress. when the stress was greater than 4GPa, it

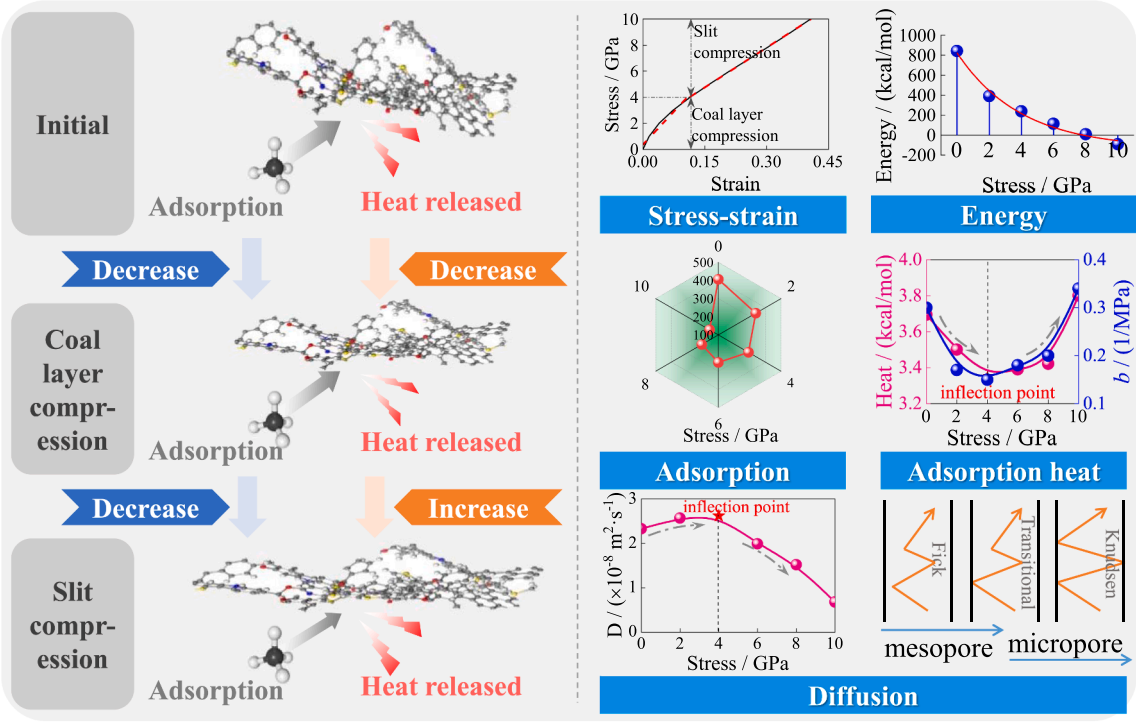

Fig. 11. Schematic diagram of CH_4 adsorption and diffusion in stressed slit framework of coal.

showed an increasing trend. During the adsorption process, the less heat was released, CH_4 is easier to be adsorbed in the framework, otherwise, the difficulty of adsorption will increase.

The diffusion type of CH_4 in the framework mainly included three parts, Knudsen, transitional and Fick diffusion. Under the action of external stress, the gas diffusion process was mainly the mutual transformation of three diffusion processes. The self-diffusion coefficient increased with the increase of the slit width. The self-diffusion coefficient of CH_4 in the framework also showed a trend of increasing first and then decreasing with the increase of stress, and the inflection point appeared when the external stress was 4 GPa. Through the calculation and analysis of the Knudsen number of the diffusion process, it was obtained that the gas diffusion was mainly the transformation process of Fick, transitional and Knudsen diffusion under various stresses in different slit framework.

Most of the above parameters changed with 4 GPa stress as the critical point. Through the analysis of the stress–strain curve of the framework, when the stress was less than 4 GPa, the main compaction occurred in the coal molecular layer. This process resulted in a rapid decrease in the energy of framework, where the difficulty of the adsorption process (which differed from the adsorption capacity of CH_4 in the framework) was decreased, the less heat was released in this process, and the diffusion of CH_4 was enhanced. When the external stress exceeded 4 GPa, the main compaction occurred in the slit. the energy in the framework showed a negative growth trend, which led to an increase in the difficulty of gas adsorption in the coal molecular layer, the heat released during the adsorption process increased, and the gas diffusion process also weakened.

4. Conclusion

(1) The deformation of coal molecular framework under external stress mainly occurred in the coal molecular layer and slit. In the initial stage of stress loading, the compression deformation mainly occurred in the coal molecular layer. Exceeding the critical stress, the slit compression deformation was the main factor. The larger the slit width, the more obvious the deformation of the framework.

(2) The energy of the framework under stress showed an exponential decay trend, which resulted in a more stable state, and the adsorption amount of CH_4 in framework also decreased. The isosteric heat of adsorption and pressure constant b of Langmuir showed a various trend of first decreasing and then increasing, indicating that the difficulty of CH_4 adsorption in the framework decreased during the compression stage of coal molecular layer. Whereas, in the slit compression stage, due to the influence of adjacent molecular layers, the difficulty of adsorption gradually increased.

(3) By quantitatively analyzing the relative concentrations of CH_4 in the coal molecular layers and slit of framework, the excess adsorption of CH_4 in the framework with different slit widths under various stresses was determined. It was worth noting that with the increase of the slit width, the excess adsorption in the coal molecular layer decreased, which was exactly opposite to the absolute adsorption in the framework.

(4) With the increase of the slit width, the self-diffusion coefficient of CH_4 in the framework shows an increasing trend. Under various stresses, the self-diffusion coefficient of CH_4 showed a various trend of first increasing and then decreasing, whose inflection point was coincided with that of adsorption heat. Through calculating the Knudsen number of the gas diffusion process, it was found that the gas diffusion type in the micropores under stress loading was mainly transitional and Knudsen diffusion, while in the mesopores, the Fick and transitional diffusion were dominant.

CRediT authorship contribution statement

Hai-fei Lin: Conceptualization, Methodology, Funding acquisition. **Hang Long:** Data analysis, Writing – original draft. **Shu-gang Li:** Writing – review & editing, Funding acquisition. **Yang Bai:** Validation. **Tong Xiao:** Appropriate words. **Ao-li Qin:** Data curation.

Declaration of Competing Interest

The authors declare that they have no known competing financial interests or personal relationships that could have appeared to influence the work reported in this paper.

Data availability

The data that has been used is confidential.

Acknowledgement

This study was financially supported by the National Natural Science Foundation of China (Nos. 51874236 and 52174207), and Shaanxi Provincial Department of Science and Technology (Nos. 2020JC-48 and 2022TD-02).

References

[1] Wang HF, Cheng YP, Wang W, et al. Research on comprehensive CBM extraction technology and its applications in China's coal mines. J Nat Gas Sci Eng 2014;20:200–7.
[2] Li LC, Wei CT, Qi Y, et al. Coalbed methane reservoir formation history and its geological control at the Shuigonghe Syncline. Arabian J Geosci 2014;8(2):619–30.
[3] Li B, Zhang JX, Ding ZB, et al. A dynamic evolution model of coal permeability during enhanced coalbed methane recovery by N_2 injection: experimental observations and numerical simulation. RSC Adv 2021;11:17249–58.
[4] Dutka B. CO_2 and CH_4 sorption properties of granular coal briquettes under in situ states. Fuel 2019;247:228–36.
[5] Zhang GJ, Li QS, Zhang Y, et al. Failure characteristics of roof in working face end based on stress evolution of goaf. Geomechanics and Geophysics for Geo-Energy and Geo-Resources 2021;7(3):1–22.
[6] Long H, Lin HF, Yan M, et al. Adsorption and diffusion characteristics of CH_4, CO_2, and N_2 in micropores and mesopores of bituminous coal: Molecular dynamics. Fuel 2021;292(1):120268.
[7] Xia YC, Rong GQ, Xing YW, et al. Synergistic adsorption of polar and nonpolar reagents on oxygen-containing graphite surfaces: Implications for low-rank coal flotation. J Colloid Interface Sci 2019;557:276–81.
[8] Han JX, Lu YJ, Makarova EY, et al. Molecular simulation of CH_4 and CO_2 competitive adsorption in moisture coals. Solid Fuel Chem 2019;53:270–9.
[9] Li Y, Yang Z, Li XG. Molecular simulation study on the effect of coal rank and moisture on CO_2/CH_4 competitive adsorption. Energy Fuels 2019;33(9):9087–98.
[10] Sharma A, Namsani S, Singh JK. Molecular simulation of shale gas adsorption and diffusion in inorganic nanopores. Mol Simul 2015;41(5–6):414–22.
[11] Zhu H, Wang W, Huo Y, et al. Molecular Simulation study on adsorption and diffusion behaviors of CO_2 / N_2 in lignite. ACS Omega 2020;5(45):29416–26.
[12] Gao D, Hong L, Wang J, et al. Molecular simulation of gas adsorption characteristics and diffusion in micropores of lignite. Fuel 2020;269:117443.
[13] Tesson S, Firoozabadi A. Methane adsorption and self-diffusion in shale kerogen and slit nanopores by molecular simulations. The Journal of Physical Chemistry C 2018;122(41):23528–42.
[14] Tolmachev AM, Anuchin KM, Fomenkov PE, et al. A molecular dynamics study of the adsorption equilibrium and density of adsorbates. J Struct Chem 2018;59:1952–9.
[15] Li SG, Bai Y, Lin HF, et al. Molecular simulation of adsorption of gas in coal slit model under the action of liquid nitrogen. Fuel 2019;255:115775.
[16] Fang SH, Zhu HQ, Gao M, et al. Evolution of pore characteristics and methane adsorption characteristics of Nanshan 1/3 coking coal under different stresses. Sci Rep 2022;12:3117.
[17] Mohammadi M, Yousefi F, Neek-Amal M, et al. Mechanical properties of twin graphene subjected to uniaxial stress by molecular dynamic simulation. Mater Res Express 2019;6(10):105611.
[18] Wu TH, Firoozabadi A. Calculation of solid-fluid interfacial free energy with consideration of solid deformation by molecular dynamics simulations. J Phys Chem A 2021;125(26):5841–8.
[19] Long H, Lin HF, Li SG, et al. Nanomechanical properties of CH_4-containing coal during CO_2 storage under different injection pressures based on molecule dynamics. Appl Surf Sci 2022;590:153126.
[20] Meng JQ, Li SC, Niu JX, et al. Effects of moisture on methane desorption characteristics of the Zhaozhuang coal: experiment and molecular simulation. Environmental Earth Sciences 2020;79(1):44.

[21] Lei HY, Tian GF, Xiao MF, et al. Application of molecular simulation in the study of polyimide. Acta Polymerica Sinica 2019;50(12):1253–62.
[22] Wiser WH, Hill GR, Kertamus NJ. Kinetic study of pyrolysis of high volatile bituminous coal. Ind Eng Chem Process Des Dev 1967;10(1):133–8.
[23] Carlson GA. Computer simulation of the molecular structure of bituminous coal. Energy Fuels 1992;6(6):771–8.
[24] Cornette V, Alexandre D, Yelpo V, et al. Binary gas mixture adsorption-induced deformation of microporous carbons by Monte Carlo simulation. J Colloid Interface Sci 2018;522:291–8.
[25] Sui HG, Yao J. Effect of surface chemistry for CH_4/CO_2 adsorption in kerogen: a molecular simulation study. J Nat Gas Sci Eng 2016;31:738–46.
[26] Meng ZP, Tian YD, Li GF. Theories and methods of coalbed methane development geology. Beijing: Science Press; 2010.
[27] Kensuke H, Masato S, Ryuta K, et al. Influence of Molecular Chain Behavior on Mechanical Properties of Poly-L-lactic Acid by Molecular Dynamics Method. Journal of the Japan Society for Composite Materials 2019;45(1):34–40.
[28] Liu XQ, He X, Qiu NX, et al. Molecular simulation of CH_4, CO_2, H_2O and N_2 molecules adsorption on heterogeneous surface models of coal. Appl Surf Sci 2016;389:894–905.
[29] Li SG, Li YJ, Yan LB, et al. Prediction of phase equilibrium of methane hydrate below 272.2 K based on different equations of state. Fluid Phase Equilib 2019;490:61–7.
[30] Zhao W, Wang K, Zhang R, et al. Influence of combination forms of intact sub-layer and tectonically deformed sub-layer of coal on the gas drainage performance of boreholes: a numerical study. International Journal of Coal Science & Technology 2020;7:571–80.
[31] Zhao T, Li X, Zhao H, et al. Molecular simulation of adsorption and thermodynamic properties on type II kerogen: Influence of maturity and moisture content. Fuel 2016;190(15):198–207.
[32] Askalany AA, Saha BB. Towards an accurate estimation of the isosteric heat of adsorption - A correlation with the potential theory. J Colloid Interface Sci 2017;490:59–63.
[33] Bai Y, Lin HF, Li SG, et al. Molecular simulation of N_2 and CO_2 injection into a coal model containing adsorbed methane at different temperatures. Energy 2021;219:119686.
[34] You XF, He M, Zhu XC, et al. Influence of surfactant for improving dewatering of brown coal: A comparative experimental and MD simulation study. Sep Purif Technol 2019;210:473–8.
[35] He XQ, Nie BS. Diffusion Mechanism of porous gases in coal seams. Journal of China University Mining and Technology 2001;30:1–4.
[36] Mastalerz M, Drobniak A, Strapoc D, et al. Variations in pore characteristics in high volatile bituminous coals: Implications for coal bed gas content. Int J Coal Geol 2008;76:205–16.